A Practical Prediction Model for Surface Deformation of Open-Pit Mine Slopes Based on Artificial Intelligence

Yankui Hao[1,*], Binbin Huang[2], Maciej Sulowicz[3]
[1]*China Coal Geology Group Co., Ltd, Beijing 100040, China*
[2]*Faculty of Mechanical Engineering, Opole University of Technology, 45-758 Opole, Poland*
[3]*Department of Electrical Engineering, Cracow University of Technology, 31-155 Cracow, Poland*
[*]*510577925@qq.com; bbhuang@qq.com; maciej.sulowicz@pk.edu.pl*

***Abstract*—To solve the problems of large prediction error, slow convergence speed, and poor generalisation ability of traditional models in predicting surface deformation of open-pit mine slopes, this paper proposes a new intelligent prediction model based on the Mayfly algorithm-optimised support vector machine (MA-SVM). In this method, the MA is used to optimise the SVM parameters to reduce the uncertainty of the model and avoid time-consuming parameter adjustment. To evaluate the proposed prediction model, real-world deformation data of the north slope of the Anjialing open-pit mine in Pingshuo city, China, are collected using the microdeformation monitoring radar and used to investigate the deformation prediction performance of the proposed method. The results of the analysis demonstrate that the proposed method is able to accurately predict the deformation of the surface of the mine slope and outperforms three existing popular methods, including SVM, genetic algorithm (GA)-SVM, and particle swarm optimisation (PSO)-SVM). The mean absolute error (MAE) of the proposed MA-SVM is 2.52 % while 6.56 %, 4.95 %, and 5.16 % for the SVM, GA-SVM, and PSO-SVM, respectively; the root mean square error (RMSE) of the proposed MA-SVM is 10.21 % while 30.79 %, 17.38 %, and 22.54 % for the other three methods. Because the proposed MA-SVM model is able to predict slope deformation using actual monitoring data, it is of practical importance in real-world applications for early warning on landslides of mine slopes.**

***Index Terms*—Deformation prediction; Mining monitoring; Artificial intelligence; Support vector machine.**

I. INTRODUCTION

Prediction of surface deformation for open-pit slopes is important in the mining safety monitoring process. Prediction accuracy is directly related to production schedule, as well as personnel and property safety. The stability of the open-pit slope is affected by many factors. The relationship between the influence factors and the slope deformations is not a linear map, but presents the characteristics of strong nonlinearities and complex uncertainties. Traditional deformation prediction methods use mathematical modelling techniques, which always consider many assumptions and simplification; as a result, the prediction accuracy is usually very low and the application range is very limited, making it difficult to meet the requirements of practical applications.

With the development of new technologies, such as artificial intelligence (AI), machine learning (ML), deep learning, and transfer learning, intelligent prediction methods have gradually become an important research and application direction for mine slope safety monitoring. For example, Fu, Wan, Fu, Xiao, Mao, and Sun [1] proposed a fuzzy method to predict the deformation of steep and high slopes based on the optimisation of all the distribution. Li and Qiu [2] combined the sparrow search algorithm (SSA) and the extreme learning machine (ELM) to predict the deformation of the slope of the Jianshan mine. Xi, Yang, Sun, and Mei [3] conducted a comparative investigation of machine learning approaches for predicting slope deformation based on monitored time-series displacement data. However, time-series forecasting often does not consider factors of influence of deformation, such as the temperature and humidity, which may decrease the effectiveness of slope deformation prediction. Therefore, it is crucial to build AI prediction models with consideration of multisource information. Moreover, currently many artificial neural network (ANN) models have been introduced for slope deformation monitoring, but most existing ANN models have problems such as slow convergence, easy to fall into local minima, and limited generalisation ability.

The support vector machine (SVM) uses structural risk minimisation in the training to avoid dimensional disaster problems and obtain reasonable generalisation ability in small sample learning, which makes it very suitable for the mine geological disaster monitoring. For example, Yang [4] combined particle swarm optimisation (PSO) and SVM to improve the prediction accuracy of slope stability. Chen, Wei, and Ma [5] built an improved ant colony algorithm (ACO)-SVM model to forecast slope displacement. Du, Song, Qu,

Manuscript received 11 January, 2024; accepted 14 May, 2024.
This research was supported by the National Natural Science Foundation of China under Grant No. U21A20107; Fundamental Research Program of Shanxi Province under Grant No. 202203021211156; Tencent Foundation or Xplorer Prize.

Zhao, Sun, and Chen [6] established a slope monitoring model using the SVM.

In recent years, the intelligent optimisation algorithm has the advantages of fast speed, high efficiency, and strong stability in parameter optimisation. With the development of high-precision deformation prediction model modelling technology, more and more scholars have introduced intelligent optimisation algorithm into the process of seeking optimal parameters of engineering slope deformation prediction model. Many factors affecting the deformation of the surface of the engineering slope, including internal factors and external factors, need to be considered during the modelling process of the engineering slope surface deformation prediction model. Through a comprehensive analysis and study of internal factors, such as geology and terrain, and induced factors, such as meteorological, earthquake, and artificial mining activities in the monitoring area, the factors that affect the deformation of the open-pit slope can be fully understood. Considering that in this study, Luzigou anticline, Anjialing reverse fault, and other structural factors have little influence on the deformation of the north slope of the study object; this paper takes the five meteorological factors and manual mining of disturbance data as the important inducing factor of the disaster to cause the deformation of the study object during the study period.

Existing literature suggests that the optimisation must be performed for the SVM to increase the running speed and enhance generalisation ability when considering multisource information. Compared to traditional optimisation algorithms, the Mayfly algorithm (MA) combines the main advantages of the swarm intelligence algorithm and evolutionary algorithm and has faster convergence speed and stronger optimisation ability [7], [8]. Therefore, in this paper, the MA is used to globally optimise the penalty factor and complexity factor of the SVM model, and a MA-SVM prediction model is constructed to predict surface deformation in a real-world open-pit slope. The prediction results indicate high precision and strong generalisability of the proposed method, which provides a new method for the prediction of slope deformation.

II. MINE SLOPE SURFACE DEFORMATION PREDICTION

A. Geological Conditions of Research Area

The Anjialing open-pit mine is located in the Pinglu district, Shuozhou City, China. It belongs to the Pingshuo mining area and is one of the three open-pit coal mines in the Pingshuo Coal Industry Co., LTD. The Pingshuo mining area belongs to the temperate semi-arid continental monsoon climate area, which presents dry, cold, and windy spring and winter while concentrated precipitation in summer and autumn with warm and cool wind. It is reported in [9] that 75 % of annual rainfall in the Pingshuo mining area is mainly in July, August, and September. The average annual temperature of the Pingshuo mining area is around 7 ℃, the daily temperature difference is 18 ℃–25 ℃, the highest temperature is 37.9 ℃, and the lowest temperature is -32.4 ℃. Due to low mountains and hills, the Shuoping area is mostly covered by the loess. The loess in the area has been subjected to strong erosion and wind cutting, and the vegetation in the area is sparse, which forms the landscape of the landform of the loess Plateau, such as beams, walls, and hills. The gully is developed in the shape of "V" with a cutting depth of 40 m to 70 m. The terrain in the region is basically high in the north and low in the south, as well as high in the middle and low in both sides. According to the digital elevation model of the slope in the north of the Anjialing slope, the research object has a highest elevation of 1,441 m, lowest elevation of 1,193 m, and the height difference between the highest and the lowest elevation is 248 m [10]. Figure 1 provides an image of the north side of the Anjialing slope.

Fig. 1. Slope topography of the north slope of the Anjialing open-pit mine. Photo taken on July 23, 2023 shows the north slope of the Anjialing open-pit mine of Pingshuo Group Co., LTD.

The open-pit slope is an artificial slope produced by coal mining. There are many factors that affect its deformation, and the relationship between them is complicated. The internal factors and the inducement factors that affect the slope deformation are analysed in [11]. Internal factors, such as formation lithology, landform, elevation, and vegetation, in the study area are relatively stable and will not change greatly in a short period of time, while induced factors, such as meteorological factors, seismic factors, and human engineering activities, will randomly occur and change the slope greatly in a short period of time, which is easy to cause slope deformation and the occurrence of disasters. Therefore, in this study, six factors affecting the deformation of the surface of the mine slope are selected as the input to the prediction model. These factors include rainfall, rainfall duration, temperature, humidity, atmospheric pressure, and human factors of mining disturbance.

B. Data Acquisition

Data collection was carried out at the Anjialing open-pit coal mine in Pingshuo for seven days in July 2023. During data collection, there was a large rainfall in the study area and a large area of deformation aggregation appeared in the monitoring area. Slope deformation continued to increase after the rainfall. Therefore, the data for deformation monitoring and meteorological influencing factors have been collected by the IBIS-M ground-based radar [12]. The IBIS-M radar is shown in Fig. 2.

The IBIS-M radar parameters were set as follows: the acquisition period was 9 min, the range-orientated resolution was 0.5 m, the angle-orientated resolution was 4.4 mrad, the minimum monitoring distance was 1.828 km, and the maximum monitoring distance was 2.633 km. The maximum monitoring distance of the IBIS-M radar is 4 km, and the

actual monitoring accuracy can reach 0.1 mm, so it can be competent for this deformation monitoring data acquisition work. The weather station (Vantage Pro2 model) is the main device on the radar to collect the meteorological data. The Vantage Pro2 includes one rain collector, one temperature sensor, one atmospheric pressure sensor, one humidity sensor, one optical sensor, and one wind meter [13], as is shown in Fig. 3. Vantage Pro2 could also meet the needs for meteorological data types and accuracy.

Fig. 2. Overview of the IBIS-M radar.

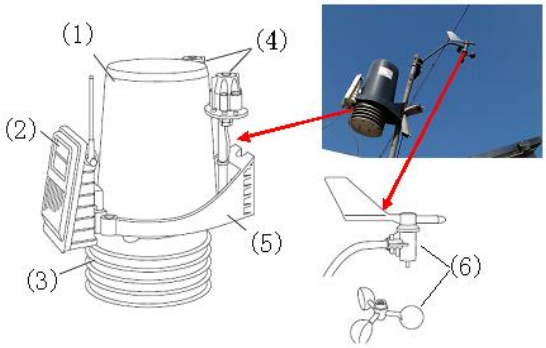

Fig. 3. Meteorological sensor module: 1 - Rain collector, 2 - Solar panel, 3 - Radiation shield, 4 - UV and Solar sensors and sensor mounting shelf, 5 - ISS base, 6 - Anemometer wane and wind cups.

The Vantage Pro2 can measure seven meteorological parameters, including rainfall, rainfall duration, temperature, atmospheric pressure, relative humidity, refractive index, wind speed, and wind direction. Considering the strong random disturbance of wind speed and direction and their small influence on mine slope deformation, they were not selected as input variables for the prediction model. In this experiment, internal factors, such as geological structure, stratum lithology, landform, elevation, and vegetation cover, in the study area are relatively stable and will not change greatly over a short period of time, while inducing factors, such as meteorological factors and human engineering activities, will occur randomly, which will have great influence and change on open-pit slope surface deformation over a short period of time. It is easy to cause slope deformation and disaster in an open-pit mine. Finally, rainfall, rainfall duration, temperature, humidity, atmospheric pressure, and human factors were selected as input data for the prediction model, and the coordinate values of the monitoring points obtained from the radial deformation data from the ground radar combined with the data from the digital elevation model of the mining area were selected as output data for the prediction model. Then the SVM-based prediction model can be established to predict the ground deformation of the mine slope considering six factors in the measured coordinate data.

III. MA-SVM PREDICTION MODEL

A. Introduction of SVM

The SVM is a kind of machine learning algorithm based on the principle of structural risk minimisation, which has great advantages in solving small samples and nonlinear high-dimensional problems [14]–[16]. The structure of the SVM for the slope deformation prediction model is shown in Fig. 4.

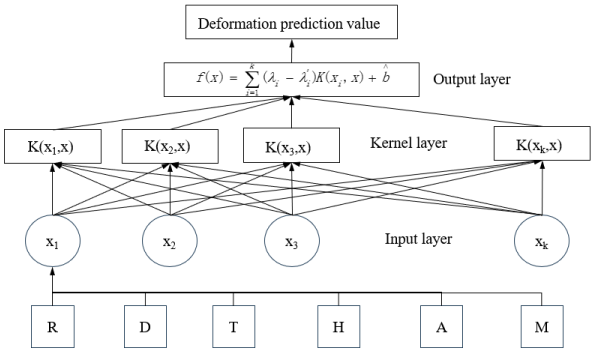

Fig. 4. SVM deformation prediction model.

The input parameters in Fig. 4 are six factors that affect the surface deformation of the open-pit slope, including rainfall (R), rainfall duration (D), temperature (T), humidity (H), atmospheric pressure (A), and human activities (M).

It can be seen from Fig. 4 that each input sample data contains relevant influencing factors that affect slope surface deformation. These six factors in input form as an input vector for the SVM. Through the kernel function and the weight of the kernel node, the support vector can be computed from the input sample vector; and then the obtained support vector passes through the output layer to generate the predicted slope deformation.

B. Mayfly Algorithm (MA)

The MA is a novel intelligent optimisation algorithm proposed by Zervoudakis and Tsafarakis in 2020 [17]. The MA optimises the target problem by simulating the flight and mating behaviour of the female and male mayflies. Hence, the MA can be considered as an improvement of the particle swarm optimisation (PSO) algorithm. Actually, the MA is an integration of the PSO, the genetic algorithm (GA), and the firefly algorithm (FA). The location of each mayfly in the search space is represented by a D-dimensional vector as a potential solution to the target problem [18]–[20]. Fitness values are represented by a predefined objective function. For the movement of the mayfly, a velocity vector is introduced [21]. The change of the flight direction of each mayfly is a dynamic interactive process. Each mayfly tends to move to the position of the individual most conducive to mating, as well as to the globally optimal position of the individual in the entire mayfly population.

The steps of MA optimisation are expressed as follows：

Step 1: Male mayfly moving.

Male mayflies move in large groups, and each male mayfly adjusts its position according to its own flying experience and the around individuals. Supposing x_i^t is the current position of the mayfly x at the time t in the search space. When summing with the velocity v_i^{t+1} at the next time step t+1, it

could get the current position at the next time step t+1, and its position update formula is

$$x_i^{t+1} = x_i^t + v_i^{t+1}, x_i^0 \in \left(x_{max}, x_{min}\right). \quad (1)$$

Considering that the male mayfly is constantly moving and performing the wedding dance on the water surface, the speed of the male mayfly v_{ij}^t in the j dimension is

$$v_{ij}^{t+1} = v_{ij}^t + a_1 e^{-\beta r_p^2}\left(p_{best,ij} - x_{ij}^t\right) + \\ + a_2 e^{-\beta r_p^2}\left(gbestj - x_{ij}^t\right), j = 1, 2..., n, \quad (2)$$

where v_{ij}^t represents the velocity value of mayfly i at the time t in the j dimension of the search space, x_{ij}^t represents the positional value of the mayfly i at the time t in the j dimension of the search space, a_1 and a_2 are used to measure the degree to which the male mayfly flight experience is less than the contribution of position, β is a fixed visibility coefficient and its default value is 2, r_p represents the current position and p_{best} represents the personal sweet spot, and r_g represents the distance between the current distance and globally optimal distance g_{best}.

The mayflies with the best current position in the population also perform the marriage dance. This motion-bit algorithm introduces a random factor, which is represented by (3)

$$v_{ij}^{t+1} = v_i^t + d \times r, \quad (3)$$

where, d is the wedding dance coefficient and r is the random number in the range [-1, 1].

Step 2: Female mayfly moving

Unlike male mayflies, female mayflies do not form groups to fly to males to reproduce.

Assuming that y_i^t is the current position of the mayfly i in the search space at time t. By summing with the velocity v_i^{t+1} at the next time step t+1, it can be obtained the current position y_i^{t+1} at time t+1, and the position update (4) can be expressed as

$$y_i^{t+1} = y_i^t + v_i^{t+1}, \quad y_i^0 \in U\left(y_{min}, y_{max}\right). \quad (4)$$

Female mayfly updates as follows

$$v_{ij}^{t+1} = \begin{cases} v_{ij}^t + a_2 e^{-\beta r_{mf}^2}\left(x_{ij}^t\right), f\left(y_i\right) > f\left(x_i\right), \\ v_{ij}^t + fl \times r, f\left(y_i\right) \le f\left(x_i\right), \end{cases} \quad (5)$$

where y_{ij}^t represents the position value of mayfly i at time t in the dimension of the search space, a_2 indicates the distance between the male and female mayflies, fl is a random walk parameter which is used to describe the random flight of the female mayflies when they are not attracted to the male mayflies.

Step 3: Mayfly mating

The crossover algorithm represents the mating process between two mayflies; one parent is selected from the male population and one from the female population. In particular, the selection can be random or based on the fitness values; if based on the fitness values, then the best female mates with the best male.

In mating behaviour, a pair of female and male mayflies produced two offspring [22]–[24]:

$$\begin{cases} o_1 = L \times m + \left(1 - L\right) \times fm, \\ o_2 = L \times fm + \left(1 - L\right) \times m, \end{cases} \quad (6)$$

where o_1 and o_2 represent two filial generations, m and fm represent the male and female mayflies, respectively, and L is a random value within a specific range [-1, 1].

C. MA-SVM Model

The radial basis function (RBF) kernel function is often used as the kernel function in the SVM model, two parameters c and γ are introduced, where c represents the penalty factor and and γ represents the complexity factor. The value of c determines the penalty degree for samples outside the error band. The complexity factor γ controls the complexity of the SVM model. The smaller the value of γ, the more complex the SVM model is. The setting of these two parameters is very important for the prediction accuracy of the SVM model. However, it takes a lot of time and energy to manually adjust these two parameters, which cannot guarantee the quality of the SVM model. Therefore, the MA algorithm is applied to optimise these two parameters to improve the accuracy of the SVM model. The flow chart of the MA-SVM prediction model proposed in this paper is illustrated in Fig. 5.

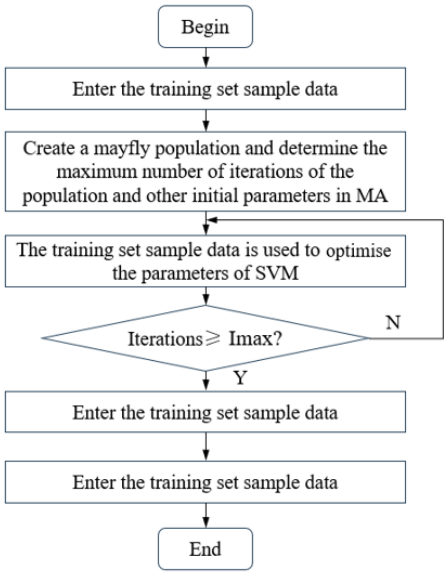

Fig. 5. Flow chart of the prediction of deformation using the MA-SVM model.

The implementation of the MA-SVM is described as follows.

Step 1: Input deformation data to train the SVM model.

Step 2: Random generation of mayfly populations; set the maximum number of iterations I_{max} of the population and other initial parameters.

Step 3: The parameters c and γ of the SVM model are optimised in the MA search space based on the prediction

error function $E(y)$ using the training set samples.

Step 4: Check whether the number of iterations reaches the maximum I_{max}. If not, repeat step 3; if reach I_{max}, the iteration is terminated and output the obtained parameters c and γ.

Step 5: Set the SVM parameters using the MA optimised ones to construct the MA-SVM prediction model.

IV. Results and Discussion

A. Overview

The prediction process for the open-pit mine slope deformation is shown in Fig. 6. First, the collected displacement data and the corresponding meteorological data from the Anjialing open-pit mine were divided into a training set and a test set after preprocessing. Second, the training set and the test data are divided into multiple data sets according to the time-series forecasting strategy. Third, existing popular AI models are established for the training data sets. Finally, the prediction accuracy of different AI models is compared using the test set. In this paper, the proposed MA-SVM model is compared with the SVM, GA-SVM, and PSO-SVM models for the slope deformation prediction.

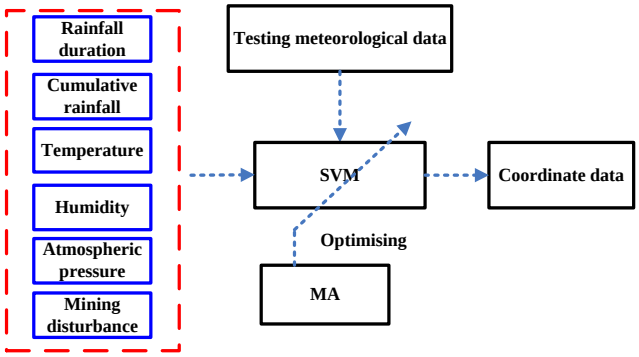

Fig. 6. The diagram of the intelligent prediction method.

B. Data Preprocessing

Daily meteorological data and the corresponding deformation monitoring records are collected and monitored at the Pingshuo, China Coal. In the monitoring data set obtained by the data collection, there are seven data types, including cumulative rainfall, rainfall duration, temperature, humidity, atmospheric pressure, human mining disturbance, and deformation coordinates of the east monitoring site. A total of 150 data sets are prepared for each type of data at the monitoring points where significant deformation occurred after the rainfall, 120 data sets are used for training the prediction model, and the rest 30 data sets are used for testing the trained prediction model. We randomly selected five groups of data from the 30 test data sets and calculated the prediction error to evaluate the prediction performance of the four AI models.

Before establishing the prediction model, it is necessary to standardise the time-series data to eliminate the influence of dimensions. In this paper, the maximum and minimum normalisation method is used to normalise the displacement data in the range of [0, 1]. The calculation method is described in (7)

$$x' = \frac{x - x_{min}}{x_{max} - x_{min}}, \tag{7}$$

where x' represents the calculated value, x_{max} is the maximum value in the sequence data, and x_{min} is the minimum in the sequence data.

C. Evaluation Indexes

Evaluation of the prediction results of the deformation monitoring models can judge the accuracy and applicability of the monitoring models. To evaluate the prediction performance of the four AI prediction models, the root mean square error (RMSE), the mean absolute error (MAE), and the mean absolute percentage error (MAPE) are adopted as evaluation indexes. The RMSE measures the degree of deviation between the predicted value and the true value and calculates the square root of the sum of squares of the difference between the predicted value and the true value. The value of the RMSE ranges from 0 to positive infinity. The smaller the value, the smaller the prediction error of the model, and the stronger the prediction ability of the model. The MAE calculates the average of the absolute values of the prediction errors for each sample. When the predicted value is exactly consistent with the real value, it is equal to 0, i.e., the prediction model is in perfect condition. The MAPE represents the average percentage of the relative error between the predicted value and the actual value. The smaller the MAPE value, the more accurate the prediction model will be.

D. Prediction Results

The prediction performance of the SVM, GA-SVM, PSO-SVM, and MA-SVM models is evaluated using the measured real-world data sets. Fig. 7(a) and 7(b) compare the values predicted by SVM, GA-SVM, PSO-SVM, and MA-SVM for the eastern site of the mine slope. The deformation values and deformation errors predicted by the four prediction models are shown in Table I and Table II. As can be seen from the results, the prediction accuracy of the MA-SVM prediction model is higher than that of the SVM, GA-SVM, and PSO-SVM prediction models. The prediction error of the MA-SVM is much smaller than that of the SVM, GA-SVM, and PSO-SVM.

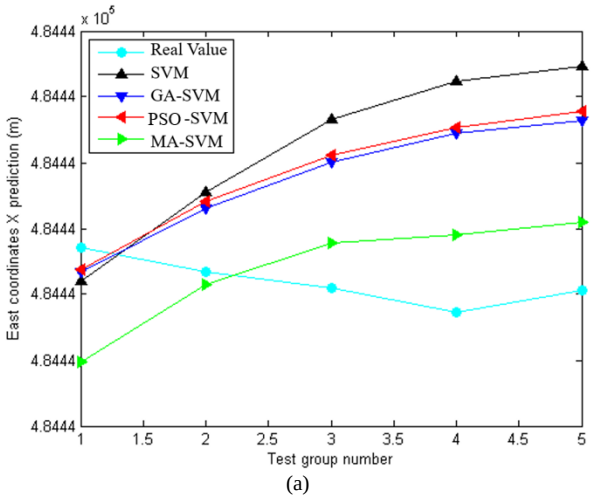

(a)

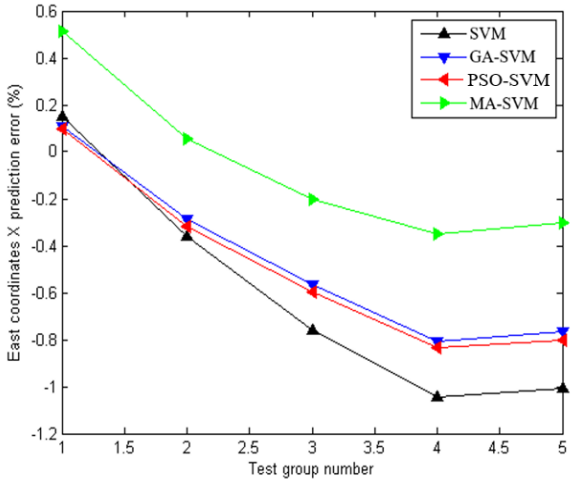

(b)

Fig. 7. Prediction performance: (a) The prediction results for the SVM, GA-SVM, PSO-SVM, and MA-SVM; (b) The prediction error for the SVM, GA-SVM, PSO-SVM, and MA-SVM.

The results show that the SVM optimised by the MA algorithm has a better training effect, a strong generalisability, and better prediction performance.

TABLE I. THE PREDICTED DEFORMATION VALUES USING THE FOUR PREDICTION METHODS.

Method	Point 1 [m]	Point 2 [m]	Point 3 [m]	Point 4 [m]	Point 5 [m]
Real value	484436.6754	484436.6747	484436.6742	484436.6734	484436.6741
SVM	484436.6744	484436.6771	484436.6793	484436.6805	484436.6809
GA-SVM	484436.6747	484436.6766	484436.6780	484436.6789	484436.6793
PSO-SVM	484436.6748	484436.6768	484436.6782	484436.6791	484436.6795
MA-SVM	484436.6719	484436.6743	484436.6756	484436.6758	484436.6762

TABLE II. THE PREDICTION ERROR USING THE FOUR PREDICTION METHODS.

Method	Point 1 [m]	Point 2 [m]	Point 3 [m]	Point 4 [m]	Point 5 [m]
SVM	0.1497	-0.3585	-0.7605	-1.0432	-1.0076
GA-SVM	0.1072	-0.2851	-0.5654	-0.8067	-0.7642
PSO-SVM	0.0960	-0.3203	-0.5976	-0.8361	-0.8022
MA-SVM	0.5133	0.0546	-0.2002	-0.3521	-0.3051

The prediction performance of the SVM prediction model depends mainly on the two parameters, the penalty factor c and the complexity factor γ. Therefore, searching for the best values of these two parameters is extremely important to improve the prediction effect of the SVM. In the training set, the GA algorithm, the PSO algorithm, and the MA algorithm are used to optimise the parameters of the SVM to find the best penalty factor c and the complexity factor γ. The optimisation process and results are shown in Figs. 8–10.

As shown in Fig. 8, the GA algorithm falls into the local optimal state at the 5th, 10th, and 20th iterations, respectively, and finally reaches the preset stop optimisation condition at the 26th iteration. As shown in Fig. 9, the PSO algorithm also falls into local optimisation at the 8th iteration, and did not reach the preset stop optimisation condition until the 13th iteration. After four iterations, the MA algorithm quickly meets the preset stop optimisation condition without falling into local optimal. As a result, MA optimisation achieved better results than the GA algorithm and the PSO algorithm.

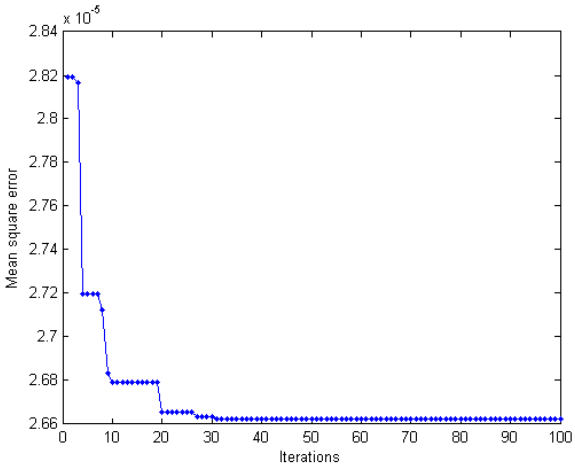

Fig. 8. Convergence curve of optimisation of the GA-SVM model.

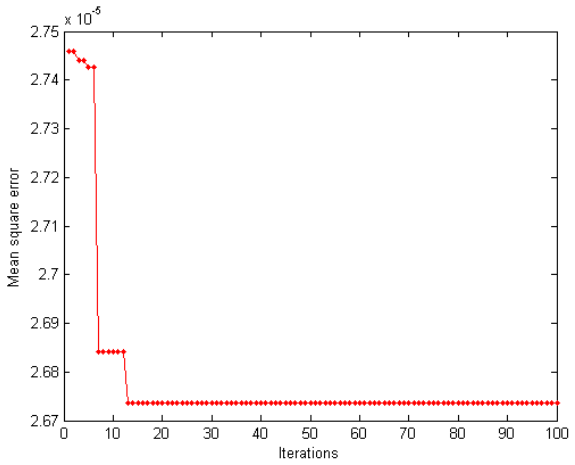

Fig. 9. Convergence curve of optimisation of the PSO-SVM model.

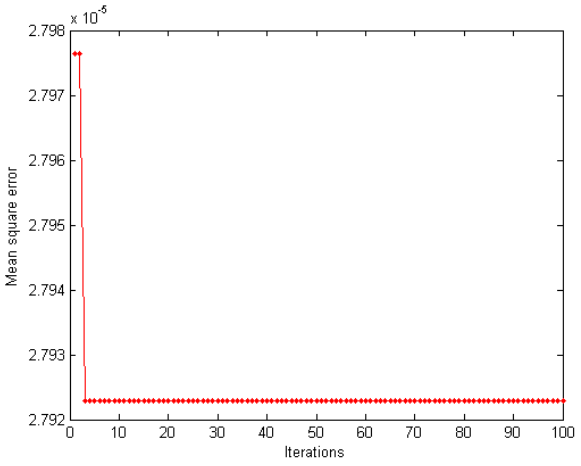

Fig. 10. Convergence curve of optimisation of the MA-SVM model.

To highlight the advantages of MA optimisation for the SVM, the surface deformation prediction models of the open-pit slope are compared using the evaluation indexes. To ensure the reliability of the test results, the test set data of the four prediction models are identical and the initial setting parameters are also the same. Table III lists the prediction errors of the four models.

TABLE III. MAE, MAPE, AND RMSE RESULTS.

Method	MAE (%)	MAPE (%)	RMSE (%)
SVM	6.56	60.54	30.79
GA-SVM	4.95	46.59	17.38
PSO-SVM	5.16	49.26	22.54
MA-SVM	**2.52**	**5.96**	**10.21**

From Table III, the prediction performance of the SVM combined with the optimisation algorithms is obviously better than that of the single use of the SVM model. The MAE, MAPE and RMSE of the MA-SVM model are respectively 2.52 %, 5.96 % and 10.21 %, which is the smallest among the four models, which indicates that the MA algorithm has improved the prediction ability of the SVM model to provide better prediction performance than that using the GA and PSO optimisation.

V. CONCLUSIONS

To improve the accuracy and generalisability of the prediction of the SVM model for the prediction of surface deformation on the open-pit mine slope, it presents the idea of using MA to optimise SVM parameters. Considering the influence of deformation factors, six factors are used to construct the SVM model, including rainfall, rainfall duration, temperature, humidity, atmospheric pressure, and human activities. Because the prediction performance of the SVM model depends mainly on the penalty factor c and the complexity factor γ, the MA is introduced to optimise these two SVM parameters. Real-world monitoring data are used to verify the proposed method and the prediction results are compared with SVM, GA-SVM and PSO-SVM. The comparison results demonstrate that the MA algorithm has stronger global search ability in the early iteration stage and stronger local search ability in the late iteration stage; the proposed MA-SVM model solves the problem of falling into local optimal solutions in the optimisation process; the prediction accuracy of the MA-SVM is superior to that of the SVM, GA-SVM and PSO-SVM models. As a result, a rapid and precise prediction of the slope surface deformation is realised using the proposed model, and the proposed MA-SVM model is feasible and practicable for predicting slope deformation in real-world mining applications.

Compared to the three models, the MA-SVM model has the best prediction accuracy and the fastest convergence speed, and can better complete the prediction task of the surface deformation of the mine slope. Compared to the SVM model (6.56 %), the GA-SVM model (4.95 %), and the PSO-SVM model (5.16 %), the proposed algorithm has the lowest mean absolute error (MAE) value (2.52 %). In terms of MAPE evaluation index, compared to the SVM model (60.54 %), the GA-SVM model (46.59 %), and the PSO-SVM model (49.26 %), the MA-SVM model (5.96 %) was also much lower than other models. In terms of RMSE evaluation indexes, compared to the SVM model (30.79 %), the GA-SVM model (17.38 %), and the PSO-SVM model (22.54 %), the MA-SVM model (10.21 %) was also much lower than other models. In terms of convergence speed, compared with the 26th iteration of the GA-SVM model and the 13th iteration of the PSO-SVM model to reach the optimal value, the model proposed in this paper only needs the 4th iteration, and the prediction time is 15.4 % and 30.8 % of the convergence time of the previous two optimisation algorithms, respectively, which is the fastest convergence speed in this paper.

In the validation of the measured data model in this paper, compared with other prediction models, MA-SVM has the following three advantages. First, the model has a higher reliability than the traditional time-series prediction model because it fully considers the factors that affect the slope deformation of the open-pit mine, including meteorological factors and human mining interference factors. Second, due to the combination of the MA optimisation algorithm and the SVM model, the model has higher prediction accuracy than the traditional model. Third, the combination of the MA optimisation algorithm and the SVM model speeds up the search process for optimal parameters. Therefore, the convergence speed of the model proposed in this paper is much lower than that of other comparison models, which improves the prediction speed of the prediction model. Fast and accurate deformation prediction is very valuable for early warning of disasters.

However, everything has two sides, so every method also has two sides. The MA-SVM prediction model proposed in this paper also has limitations and deficiencies. Due to the limitations of experimental conditions, it fails to fully consider other factors, such as the physical properties of rock and soil slopes and other disaster formation factors. However, the application of this method has a certain premise; through the study of the factors influencing slope deformation in the study area, the internal factors affecting the slope are analysed, the internal factors, such as formation lithology, topography, elevation, and vegetation cover, are relatively stable and will not change much in a short time. Therefore, only meteorological factors and human engineering activities are taken into account and the influence of them on slope deformation and the occurrence of disasters in open-pit is considered in a short time.

VI. FUTURE WORK

To improve the prediction accuracy and spatial resolution of the prediction data of the deformation prediction model in the open-pit slope surface deformation prediction model and give full play to the prediction and early warning function of the deformation prediction model, further research work will be carried out in the following three aspects.

1. The most effective way to improve the prediction accuracy of the deformation prediction model is to reduce the monitoring error from the source of the training data set. Improving the accuracy of ground-based interference radar and meteorological sensor deformation monitoring data can effectively improve the accuracy of the prediction model. In addition, the data acquisition accuracy of the meteorological sensor in this paper can also effectively improve the accuracy of the prediction model.
2. To improve the spatial resolution of the deformation prediction model, the accuracy of surface mine slope disaster deformation prediction and prediction is related to the distribution location and distribution density of meteorological observation stations, the accuracy of meteorological data prediction, the accuracy of digital elevation model (DEM), the degree of disaster geological survey, and other aspects. If further improvement is necessary to improve the accuracy of deformation

prediction and prediction, the accuracy and detail of the above-related factors must be improved.

3. The open-pit slope surface deformation prediction model should be combined with other deformation monitoring equipment in practical application. The deformation prediction model proposed in this paper has some technical limitations, such as monitoring range, single-point monitoring accuracy, image data matching, and other problems. Other deformation monitoring technologies, such as InSAR, GPS, and 3D laser scanners and manual field inspection mechanisms, should be assisted to maximise their monitoring utilisation and accuracy.

Therefore, how to minimise and reduce the monitoring errors of various monitoring data from the original data, improve the collection density and spatial resolution of various monitoring data, and combine the practical application of a variety of other advanced monitoring equipment and manual inspection to cooperate with the prediction model, is the future development trend and hot spot of surface deformation prediction model application research of open-pit slope.

CONFLICTS OF INTEREST

The authors declare that they have no conflicts of interest.

REFERENCES

[1] Y. Fu, L. Wan, X. Fu, D. Xiao, Y. Mao, and X. Sun, "A deformation forecasting model of high and steep slope based on fuzzy time series and entire distribution optimization", *IEEE Access*, vol. 8, pp. 176112–176121, 2020. DOI: 10.1109/ACCESS.2020.3027206.

[2] B. Li and J. Qiu, "Displacement prediction of open-pit mine slope based on SSA-ELM", *Front. Earth Sci.*, vol. 11, p. 1126394, 2023. DOI: 10.3389/feart.2023.1126394.

[3] N. Xi, Q. Yang, Y. Sun, and G. Mei, "Machine learning approaches for slope deformation prediction based on monitored time-series displacement data: A comparative investigation", *Appl. Sci.*, vol. 13, no. 8, p. 4677, 2023. DOI: 10.3390/app13084677.

[4] J. Yang, "Slope stability prediction based on adaptive CE factor quantum behaved particle swarm optimization-least-square support vector machine", *Front. Earth Sci*., vol. 11, p. 1098872, 2023. DOI: 10.3389/feart.2023.1098872.

[5] J. Chen, Y. Wei, and X. Ma, "Forecasting slope displacement of the agricultural mountainous area based on the ACO-SVM model", *Comput. Intell. Neurosci.*, vol. 2022, p. 2519035, 2022. DOI: 10.1155/2022/2519035.

[6] S. Du, R. Song, Q. Qu, Z. Zhao, H. Sun, and Y. Chen, "Surface deformation prediction model of high and steep open-pit slope based on APSO and TWSVM", *Elektronika ir Elektrotechnika*, vol. 30, no. 1, pp. 77–83, 2024. DOI: 10.5755/j02.eie.36115.

[7] Q. Du and H. Zhu, "Dynamic elite strategy mayfly algorithm", *PLOS One*, vol. 17, no. 8, p. e0273155, 2023. DOI: 10.1371/journal.pone.0273155.

[8] Z. Yan, J. Yan, Y. Wu, and C. Zhang, "An improved hybrid mayfly algorithm for global optimization", *J. Supercomput.*, vol. 79, no. 6, pp. 5878–5919, 2023. DOI: 10.1007/s11227-022-04883-9.

[9] S. Shi, Z. Guo, P. Ding, Y. Tao, H. Mao, and Z. Jiao, "Failure mechanism and stability control technology of slope during open-pit combing underground extraction: A case study from Shanxi Province of China", *Sustainability*, vol. 14, no. 14, p. 8939, 2022. DOI: 10.3390/su14148939.

[10] Q.-L. Ding, Y.-Y. Peng, Z. Cheng, and P. Wang, "Numerical simulation of slope stability during underground excavation using the Lagrange element strength reduction method", *Minerals*, vol. 12, no. 8, p. 1054, 2022. DOI: 10.3390/min12081054.

[11] X. Liu, M. Jing, and Z. Bai, "Heavy metal concentrations of soil, rock, and coal gangue in the geological profile of a large open-pit coal mine in China", *Sustainability*, vol. 14, no. 2, p. 1020, 2022. DOI: 10.3390/su14021020.

[12] C. Michel and S. Keller, "Advancing ground-based radar processing for bridge infrastructure monitoring", *Sensors*, vol. 21, no. 6, p. 2172, 2021. DOI: 10.3390/s21062172.

[13] A. P. Chaikovsky *et al.*, "Synergy of ground-based and satellite optical remote measurements for studying atmospheric aerosols", *J. Appl. Spectrosc*., vol. 86, no. 6, pp. 1092–1099, 2020. DOI: 10.1007/s10812-020-00945-z.

[14] Y. Liu, X. Ren, J. Zhang, and Y. Zhang, "Application and comparison of machine learning algorithms for predicting rock deformation in hydraulic tunnels", *Math. Probl. Eng.*, vol. 2022, p. 6832437, 2022. DOI: 10.1155/2022/6832437.

[15] Y. Zhang, S. Tian, W. Gong, C. Zhao, and H. Tang, "Adaptive interval prediction method for step-like landslide displacement with dynamic switching between different deformation states", *B. Eng. Geol. Environ.*, vol. 82, no. 11, art no. 403, 2023. DOI: 10.1007/s10064-023-03418-7.

[16] C. Wang and W. Guo, "Prediction of landslide displacement based on the variational mode decomposition and GWO-SVR model", *Sustainability*, vol. 15, no. 6, p. 5470, 2023. DOI: 10.3390/su15065470.

[17] D. Zhou, Z. Kang, X. Su, and C. Yang, "An enhanced Mayfly optimization algorithm based on orthogonal learning and chaotic exploitation strategy", *Int. J. Mach. Learn. Cyb*., vol. 13, no. 11, pp. 3625–3643, 2022. DOI: 10.1007/s13042-022-01617-4.

[18] T. Bhattacharyya, B. Chatterjee, P. K. Singh, J. H. Yoon, Z. W. Geem and R. Sarkar, "Mayfly in harmony: A new hybrid meta-heuristic feature selection algorithm", *IEEE Access*, vol. 8, pp. 195929–195945, 2020. DOI: 10.1109/ACCESS.2020.3031718.

[19] Y. Zhao, C. Huang, M. Zhang, and C. Lv, "COLMA: A chaos-based mayfly algorithm with opposition-based learning and Levy flight for numerical optimization and engineering design", *J. Supercomput*., vol. 79, no. 17, pp. 19699–19745, 2023. DOI: 10.1007/s11227-023-05400-2.

[20] G. Natesan, S. Konda, R. Perez de Prado, and M. Wozniak, "A hybrid Mayfly-Aquila optimization algorithm based energy-efficient clustering routing protocol for wireless sensor networks", *Sensors*, vol. 22, no. 17, p. 6405, 2022. DOI: 10.3390/s22176405.

[21] K. Zervoudakis and S. Tsafarakis, "A mayfly optimization algorithm", *Comput. Ind. Eng.*, vol. 145, art. 106559, 2020. DOI: 10.1016/j.cie.2020.106559.

[22] A. Zou, L. Wang, W. Li, J. Cai, H. Wang, and T. Tan, "Mobile robot path planning using improved mayfly optimization algorithm and dynamic window approach", *J. Supercomput.*, vol. 79, no. 8, pp. 8340–8367, 2023. DOI: 10.1007/s11227-022-04998-z.

[23] G. Lei, X. Chang, Y. Tianhang, and W. Tuerxun, "An improved mayfly optimization algorithm based on median position and its application in the optimization of PID parameters of hydro-turbine governor", *IEEE Access*, vol. 10, pp. 36335–36349, 2022. DOI: 10.1109/ACCESS.2022.3160714.

[24] H. Hu, H. Li, G. Liang, L. Zhao, J. Yang, and X. Wei, "Phase-only pattern synthesis for spaceborne array antenna based on Improved Mayfly Optimization Algorithm", *Electronics*, vol. 12, no. 4, p. 895, 2023. DOI: 10.3390/electronics12040895.